Journal of The Electrochemical Society, 2023 **170** 011504

Calculation of Cathodic Limiting Current Density in Weak Acids: Part I. Aqueous CO_2 Solutions

Srdjan Nesic[1] **and Fazlollah Madani Sani**[1,*,z]

Institute for Corrosion and Multiphase Technology, Department of Chemical and Biomolecular Engineering, Ohio University, Athens, OH 45701, United States of America

The limiting current density for the hydrogen evolution reaction in aqueous saturated carbon dioxide solutions needed revisiting, as the basic understanding of the underlying reaction mechanism in weak acids has changed over the past few years. We now know that the direct reduction of undissociated carbonic acid on a metal surface in aqueous carbon dioxide solutions is not significant, as was thought before, and that there is only a single dominant pathway for hydrogen evolution: reduction of free hydrogen ions. The main role of weak carbonic acid is to provide additional hydrogen ions via buffering. Therefore, a new mathematical model was needed for calculation of the limiting current density for hydrogen ion reduction, that accounts for both hydrogen ion diffusion in the boundary layer and simultaneous buffering provided by dissociation of weak carbonic acid. The new model relies on analytically solving the co-diffusion of hydrogen ions and carbonic acid in the mass transfer boundary layer, with simultaneous homogenous chemical reactions. The new expression for the limiting current density takes the form:

$$i_{lim,\,H^+}^{buff,CO_2} = F\sqrt{D_{H^+}^{eff,CO_2}\, k_{f,\,CO_2}\, c_{b,CO_2}^{eq}\, c_{b,H^+}^{eq}}\, coth\left(\frac{\delta_{m,\,H^+}}{\delta_{r,\,H^+}^{CO_2}}\right)$$

The performance of the new model was successfully validated by comparing it with experimental data over a broad range of conditions.

 [DOI: 10.1149/1945-7111/acb4e5]

Manuscript submitted September 8, 2022; revised manuscript received January 16, 2023. Published February 1, 2023.

When a reaction other than charge transfer in a multistep cathodic reaction sequence is *slow* and becomes the rate determining step (*rds*), this leads to the concept of *limiting reaction rate* or *limiting current density*.[1] The term limiting current density was first introduced by Brunner;[2] for a given cathodic reaction, the limiting current density is the maximum attainable current density and is of great practical importance in several fields such as (electro)chemistry, electroplating, electrodialysis, battery research, corrosion studies, *etc*. That slow step can be mass transfer by diffusion of species between the bulk solution and the surface or a preceding homogenous chemical reaction producing species close to the surface. Either way, the electroactive species involved in the cathodic reaction are in short supply at the metal (electrode) surface and the rate of the charge transfer process is limited, and so is the rate of the overall cathodic reaction. The slow step can also be crystallization, for example: inclusion of adsorbed metallic ions into the crystal lattice;[3] however, crystallization limiting current densities are associated primarily with reductive metal deposition, and will not be discussed in this paper. The primary focus of this article is the rate of a heterogeneous electrochemical reaction at a metal surface limited by a diffusion process coupled with a preceding linear homogenous chemical reaction.

Buffered electrolytic solutions such as aqueous solutions of weak acids are examples of systems where the rate of a heterogeneous electrochemical reaction is affected by a slow preceding homogenous chemical reaction step. We will start here with an example of an aqueous CO_2 solution, where weak carbonic acid, H_2CO_3 forms and acts as a buffer. Other weak acids such as aqueous hydrogen sulfide and aqueous solutions of organic acids behave similarly, but all have their specificities; hence, they will be covered in separate publications.

Aqueous CO_2-saturated solutions are very common, particularly in the oil and gas industry, where some water and gaseous CO_2 emerge with the produced hydrocarbons. The aqueous CO_2-saturated solutions can cause significant internal corrosion problems for mild steel pipelines transporting the production stream to processing facilities. Another corrosion problem caused by these solutions is related to CO_2 capture, transportation, and storage equipment and facilities, when small amounts of water are present in the dense CO_2 phase. Being able to model the behavior of the cathodic reaction, which its rate governs the corrosion rate of mild steel exposed to aqueous CO_2 solutions is of extreme importance in protecting mild steel equipment against corrosion.[4–8]

The diprotic H_2CO_3 is produced by a *slow* homogenous chemical reaction—hydration of aqueous CO_2, according to:

$$CO_{2(aq)} + H_2O_{(l)} \underset{k_{b,CO_2}}{\overset{k_{f,CO_2}}{\rightleftarrows}} H_2CO_{3(aq)} \qquad [1]$$

which dissociates partially, via a relatively *fast* reaction:

$$H_2CO_{3(aq)} \underset{k_{b,H_2CO_3}}{\overset{k_{f,H_2CO_3}}{\rightleftarrows}} HCO_{3(aq)}^- + H_{(aq)}^+ \qquad [2]$$

The bicarbonate ion, HCO_3^- is a much weaker acid ($pK_{HCO_3^-} \approx 10.3$ at 25 °C) when compared to H_2CO_3 (with a $pK_{H_2CO_3} \approx 3.7$ at 25 °C), so its dissociation and the effect on buffering in aqueous CO_2saturated solutions can be usually ignored.

The H^+ ions, produced by the homogenous dissociation Reaction 2 in the bulk, diffuse and adsorb onto the metal surface:

$$H_{(aq)}^+ \overset{diffusion}{\rightarrow} H^+|_{surface} \qquad [3]$$

At the surface, the adsorbed H^+ ions are reduced to evolve hydrogen gas according to:

$$H^+|_{surface} + e^- \rightarrow \frac{1}{2}H_{2(g)} \qquad [4]$$

Reaction 4 is actually a multistep electrochemical reaction,[1,9,10] a combination of diffusion and homogenous chemical reaction in the

*Electrochemical Society Member.
[z]E-mail: fm874012@ohio.edu

bulk solution and charge transfer at the metal surface. In the present article, the focus is on the calculation of the limiting current density for Reaction 4, which is governed jointly by diffusion and homogenous chemical reaction processes in the bulk solution. Therefore, the charge transfer process at the metal surface does not impact the limiting current density calculation.

The overall hydrogen evolution reaction in aqueous CO_2 saturated solutions is then obtained as a summation of all abovementioned steps:

$$CO_{2(aq)} + H_2O_{(l)} + e^- \rightarrow HCO^-_{3(aq)} + \frac{1}{2}H_{2(g)} \quad [5]$$

Since the mid-1970's and the pioneering work of deWaard and Milliams,[4,11] it has been assumed that, in addition to the hydrogen ion reduction, Reaction 4, there is a parallel hydrogen evolution reaction—the so-called direct reduction of carbonic acid:

$$H_2CO_{3(aq)} + e^- \rightarrow HCO^-_{3(aq)} + \frac{1}{2}H_{2(g)} \quad [6]$$

which is responsible for higher limiting current densities seen in the weak carbonic acid solutions compared to strong acid solutions at the same pH. However, over the past decade, it has been demonstrated that this parallel reaction pathway is nonexistent/insignificant and that the main role of weak H_2CO_3 is to act as a buffer, and provide additional H^+ ions, when molecular diffusion cannot keep up.[7,12,13] This happens only when the charge transfer Reaction 4 proceeds so quickly that the rate of the overall reaction is limited by the ability to provide the H^+ ions to the metal surface. It has also been shown that the presence of aqueous CO_2 and weak H_2CO_3 acid, does not affect significanlty the rate of charge transfer process in the hydrogen evolution reaction.[7,13]

In the past, when the assumption about two independent cathodic Reactions 4 and 6 was considered to be valid, calculating a limiting current density was a relatively straightforward task. First, a pure mass transfer limiting current density i^{diff}_{lim,H^+} was calculated for the H^+ ion reduction Reaction 4:

$$i^{diff}_{lim,H^+} = \frac{F\, D_{H^+}\, c_{b,H^+}}{\delta_{m,H^+}} = F\, k_{m,H^+} c_{b,H^+} \quad [7]$$

where F is the Faraday constant, D_{H^+} is the diffusivity of H^+ ions, c_{b,H^+} is the bulk concentration of H^+ ions, δ_{m,H^+} is the thickness of the mass transfer boundary layer and k_{m,H^+} is the mass transfer coefficient of H^+ ions, all referring to an aqueous solution.[6,14,15]

Then, the limiting current density for the direct reduction of H_2CO_3, Reaction 6, was calculated by assuming that the rate of reduction of H_2CO_3 is controlled by the slow hydration Reaction 1, producing H_2CO_3 near the metal surface. Following Vetter's original derivation[3] for stagnant solutions and a modification introduced by Nesic et al.[15] for flowing solutions, the limiting current density for the direct carbonic acid reduction i^{chem}_{lim,H_2CO_3} was calculated via:

$$i^{chem}_{lim,H_2CO_3} = F\, c^{eq}_{b,H_2CO_3} \sqrt{D_{H_2CO_3} k_{b,CO_2}}\; coth\left(\frac{\delta_{m,H_2CO_3}}{\delta_{r,H_2CO_3}}\right) \quad [8]$$

where c^{eq}_{b,H_2CO_3} is the bulk concentration of H_2CO_3, $D_{H_2CO_3}$ is the diffusivity of H_2CO_3, $k_{b,\,CO_2}$ is the backward reaction rate constant for Reaction 1, $\delta_{m,\,H_2CO_3}$ and $\delta_{r,\,H_2CO_3}$ are the mass transfer and chemical reaction boundary layer thicknesses, respectively, all referring to an aqueous solution. Note that $\delta_{m,\,H_2CO_3}$ and $\delta_{r,\,H_2CO_3}$ were defined different in the original Nesic et al.[15] publication compared to what is shown below.

Finally, the two limiting current densities (7) and (8) for the two Reactions 4 and 6, respectively, were simply added to obtain the total cathodic limiting current density in aqueous CO_2saturated solutions.

$$i^{tot}_{lim} = i^{diff}_{lim,H^+} + i^{chem}_{lim,H_2CO_3} = \frac{F\, D_{H^+} c_{b,H^+}}{\delta_{m,H^+}} + F\, c^{eq}_{b,H_2CO_3} \sqrt{D_{H_2CO_3} k_{b,CO_2}}\, coth\left(\frac{\delta_{m,H_2CO_3}}{\delta_{r,H_2CO_3}}\right) \quad [9]$$

The calculated values for i^{tot}_{lim} seemed to agree rather well with measured limiting current densities in CO_2 solutions, reinforcing the idea that there were two parallel electrochemical reactions for hydrogen evolution in aqueous CO_2 solutions.

Now that we know there is only one main cathodic reaction, Reaction 4, the question then arises as to how accurately calculate the limiting current density and account for both diffusion of H^+ ions and simultaneous buffering provided by dissociation of H_2CO_3 in Reaction 2. This is the subject of the derivation presented below.

Calculation of the Cathodic Limiting Current Density in Aqueous CO_2-Saturated Solutions

To be able to calculate the limiting current density with only one reaction (H^+ ion reduction reaction), we will now postulate a model for diffusion of H^+ ions, Reaction 3, in the presence of buffering by the homogenous chemical Reaction 2, where H^+ ions are replenished as they are consumed by the charge transfer Reaction 4. We will assume that conditions are such that the charge transfer Reaction 4 proceeds so quickly that the overall reaction rate is limited by H^+ ion diffusion in the presence of buffering; this happens at more negative potentials *vs.* the open circuit potential of the metal surface, *i.e.*, in the limiting current density region. However, it is also known that the hydration Reaction 1 is the slowest step (*rds*) in the multistep reaction sequence mentioned above; therefore, the following dissociation step, Reaction 2, which is much faster can be considered to be almost in equilibrium.

In the limiting current density scenario, it is clear that as the metal surface is being approached, the concentration of H^+ ions decreases toward zero, but so does the concentration of H_2CO_3, which is in equilibrium with H^+ ions, due to the relatively fast dissociation step, Reaction 2. Therefore, we cannot ignore the diffusion of H_2CO_3 towards the metal surface, which occurs simultaneously with diffusion of H^+ ions. Hence, now we have to resolve a case of co-diffusion of H^+ and H_2CO_3.[16,17]

The question is what happens to the other aqueous species in the mass transfer boundary layer. To make the following derivations manageable, we will here assume that the concentration of aqueous carbon dioxide in the diffusion boundary layer, c_{CO_2} is constant and equal to the equilibrium value found in the bulk. This is based on an argument originally presented by Vetter's[3] for a similar problem involving acetic acid. In the present case, we can argue that c_{CO_2} is usually much higher than either c_{H^+} or $c_{H_2CO_3}$ so that the changes in c_{CO_2} in the diffusion boundary layer due to Reaction 1 are so small that they can be ignored. Thus, we can write:

$$c_{CO_2} \approx c^{eq}_{b,CO_2} = \text{constant} \quad [10]$$

Assuming that c_{CO_2} is constant, implies that diffusion of CO_2 in the diffusion boundary layer can be ignored in the calculations of the limiting current density.

We need to make another similar assumption to simplify the derivations: that the concentration of the bicarbonate ion in the diffusion boundary layer, $c_{HCO_3^-}$ can also be considered to be constant and equal to the equilibrium value found in the bulk. This is also following Vetter's line of reasoning:[3] when $c_{HCO_3^-}$ is much higher than either c_{H^+} and $c_{H_2CO_3}$, then the changes in $c_{HCO_3^-}$ are relatively small and can be ignored. So, we can write:

$$c_{HCO_3^-} \approx c^{eq}_{b,HCO_3^-} = \text{constant} \quad [11]$$

The assumption about constant $c_{HCO_3^-}$ allows us to ignore the contribution of HCO_3^- diffusion in limiting current density calculations. Based on a similar argument, the changes in hydroxide ions concentration, c_{OH^-} and its diffusion can be also ignored.

To determine the practical range of validity for these assumptions in typical aqueous CO_2 systems, one can look at the aqueous speciation diagrams calculated for an open system (where partial pressure of CO_2 is constant and equal to 1 bar) and a closed system (where the total amount of carbonic species is constant), shown in Fig. 1. There, the assumption about high c_{CO_2} is valid for pH2 and higher; the upper limit for a closed system is at around pH6 and there is none for an open system, which is more common in practice. The assumption about high $c_{HCO_3^-}$ is valid for pH4 and higher at 1 bar CO_2. For CO_2 partial pressures above 1 bar, the lower pH threshold moves to lower pH and vice versa. Therefore, we can conclude that these assumptions hold for many practical situations, say in aqueous CO_2 corrosion of mild steel, where the typical pH range is $5 < pH < 6$ and the partial pressure of CO_2 is of the order of 1 bar or higher.[16,17]

It needs to be pointed out here that these kinds of simplifying assumptions are absolutely necessary in order to solve the resulting transport equations analytically, as originally demonstrated by Vetter.[3] Actually, most other similar analytical developments, e.g., Koutecky and Levich,[18] Dogonadze,[19] Rieger,[20] Leal *et al.* 2018[21] and 2020[22] also considered two generic species diffusing (usually denoted as A and B) to find an analytical solution to the problem. When more species needed to be considered, the only option was to use numerical methods to solve the governing equations, as recently demonstrated by Harding et al.[23]

When formulating the transport equations for the two species that need to be solved, we will ignore mass transfer by both convection and (electro)migration and assume one-dimensional diffusion along the x-axis perpendicular to the metal surface. The justification for this assumption is as follows: the effect of convection in the boundary layer can be ignored for flow systems where there are no fluid velocity components (*i.e.*, no convection) in the direction perpendicular to the metal surface. This is a perfectly suitable approximation for the case of turbulent mass transfer in a boundary layer formed at the interface of a metal surface. A very common example is found in turbulent pipe flow, but also other similar turbulent flow systems, in both laboratory and practice, such as: turbulent rotating cylinder flow, turbulent flow in a channel, etc. It needs to be pointed out that this simplifying assumption does not appear to be valid for some other frequently encountered laboratory flow systems, such as laminar rotating disc flow, laminar impinging jet flow, etc., where the contribution of the convection of species perpendicular to the surface cannot be ignored. The mathematical treatment of such systems is more complicated as originally shown by Dogonadze,[19] then followed by Hale,[24] Leal et al.,[21] etc. However, it will be shown in the validation section below, that once the laminar boundary layer thickness is estimated for such laminar flow geometries, the approach shown here still provides reasonable predictions for the limiting current density. The other assumption about ignoring electro(migration) also holds for turbulent boundary layers, given that usually there is no externally applied electrical field. This leaves us only with one-dimensional molecular diffusion as the main mass transfer mechanism.

Now we are in the position to formulate the model by writing the steady-state one-dimensional *Nernst-Planck* equation for the two remaining species: H^+ ions and H_2CO_3; the so-called co-diffusion equations are:

$$\frac{d}{dx}\left(D_{H^+}\frac{\partial c_{H^+}}{\partial x}\right) + k_{f,H_2CO_3}c_{H_2CO_3} - k_{b,H_2CO_3}c_{H^+}c_{HCO_3^-} = 0 \quad [12]$$

$$\frac{d}{dx}\left(D_{H_2CO_3}\frac{\partial c_{H_2CO_3}}{\partial x}\right) + k_{f,CO_2}c_{CO_2} - k_{b,CO_2}c_{H_2CO_3} - k_{f,H_2CO_3}c_{H_2CO_3} + k_{b,H_2CO_3}c_{H^+}c_{HCO_3^-} = 0 \quad [13]$$

where, x is the distance from the metal surface.

The first term in both equations is the molecular diffusion term, while the other terms denote production and consumption of species due to chemical reactions. The magnitude of the chemical reaction terms is obtained with respect to Reactions 1 and 2.

As explained above, there are various techniques that can be used to solve the co-diffusion equations, Eqs. 12 and 13, some of them analytical and others numerical.[12,18,20,25–30] The numerical techniques are generally effective but do not result in explicit expressions that can be readily used in electrochemical models. On the other hand, the existing analytical methods[3,18–20,28–30] proposed in the past cannot cope with the chemical reaction terms such as those given in Eqs. 12 and 13. A new analytical approach is proposed here.

In order to solve co-diffusion Eqs. 12 and 13 in the present approach, we will start by adding them up so that some of the chemical reaction kinetic terms cancel out each other.[20]

$$D_{H^+}\frac{d^2c_{H^+}}{dx^2} + D_{H_2CO_3}\frac{d^2c_{H_2CO_3}}{dx^2} + k_{f,CO_2}c^{eq}_{b,CO_2} - k_{b,CO_2}c_{H_2CO_3} = 0 \quad [14]$$

In this step, we have used the assumptions about c_{CO_2} being constant and equal to the bulk value and then assumed that

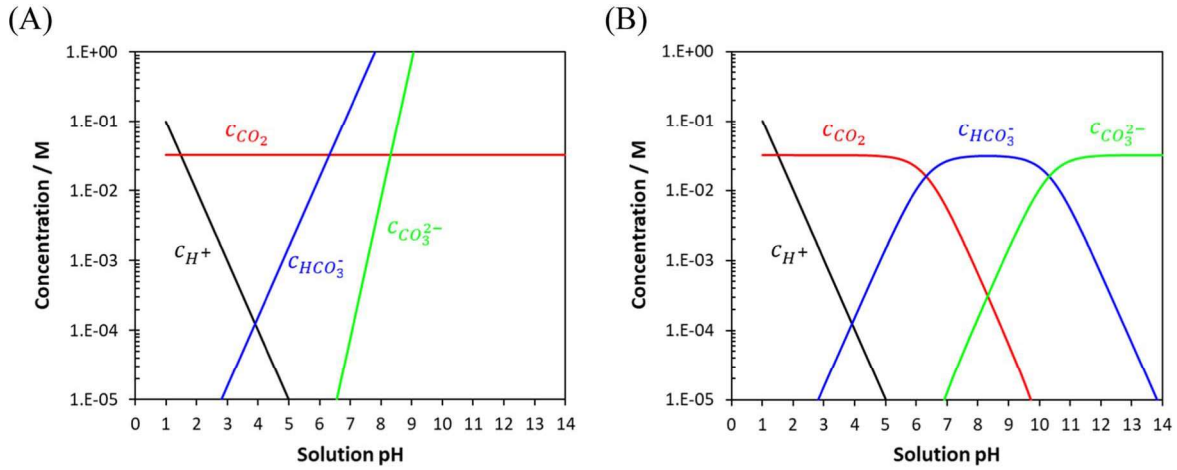

Figure 1. Distribution of dissolved species in an aqueous CO_2 solution at 25 °C and partial pressure of ~1 bar CO_2 in (A) an open system (where partial pressure of CO_2 is constant) and (B) a closed system (where the total amount of carbonic species is constant). Calculations performed using the Oddo and Tomson model [34] for an ideal solution.

diffusivities, D_{H^+} and $D_{H_2CO_3}$ are constant throughout the mass transfer boundary layer.

Now, we will relate the concentration of H_2CO_3 to that of H^+ ions. Given that the dissociation Reaction 2 is near equilibrium, we can write:

$$c_{H_2CO_3} \approx \frac{c^{eq}_{b,HCO_3^-}}{K_{H_2CO_3}} c_{H^+} \quad [15]$$

where $K_{H_2CO_3}$ is the equilibrium constant for Reaction 2. Then, by differentiating two times with respect to x, we get:

$$\frac{d^2 c_{H_2CO_3}}{dx^2} \approx \frac{c^{eq}_{b,HCO_3^-}}{K_{H_2CO_3}} \frac{d^2 c_{H^+}}{dx^2} = \frac{c^{eq}_{b,H_2CO_3}}{c^{eq}_{b,H^+}} \frac{d^2 c_{H^+}}{dx^2} \quad [16]$$

In this differentiation, we have used the assumption about $c_{HCO_3^-}$ being constant and equal to the bulk value. Eqs. 15 and 16 can be used to eliminate $c_{H_2CO_3}$ from the co-diffusion Eq. 14, to get:

$$\left(D_{H^+} + \frac{c^{eq}_{b,H_2CO_3}}{c^{eq}_{b,H^+}} D_{H_2CO_3} \right) \frac{d^2 c_{H^+}}{dx^2} + k_{f,CO_2} c^{eq}_{b,CO_2} - \frac{k_{b,CO_2}\, c^{eq}_{b,HCO_3^-}}{K_{H_2CO_3}} c_{H^+} = 0 \quad [17]$$

The first term in the parentheses on the left-hand side of Eq. 17 can be defined as *effective diffusivity* of H^+ ions in the presence of aqueous CO_2, which accounts for co-diffusion:

$$D^{eff,CO_2}_{H^+} = D_{H^+} + \frac{c^{eq}_{b,H_2CO_3}}{c^{eq}_{b,H^+}} D_{H_2CO_3} \quad [18]$$

Equation 17 can be further simplified by making use of the equilibrium expression for Reaction 1, that is, the forward rate is equal to the backward rate:

$$k_{f,CO_2}\, c^{eq}_{b,CO_2} = k_{b,CO_2}\, c^{eq}_{b,H_2CO_3} \quad [19]$$

Then, we can transform the co-diffusion Eq. 17 to read:

$$D^{eff,CO_2}_{H^+} \frac{d^2 c_{H^+}}{dx^2} + k_{b,CO_2} c^{eq}_{b,H_2CO_3} \left(1 - \frac{c^{eq}_{b,HCO_3^-}}{K_{H_2CO_3}\, c^{eq}_{b,H_2CO_3}} c_{H^+} \right) = 0 \quad [20]$$

We can also utilize the equilibrium expression for Reaction 2:

$$K_{H_2CO_3} = \frac{c^{eq}_{b,HCO_3^-}\, c^{eq}_{H^+}}{c^{eq}_{H_2CO_3}} \quad [21]$$

and now we can see that the fraction term shown in the parenthesis in Eq. 20 is equal to the reciprocal of the equilibrium (bulk) concentration of H^+ ions, c^{eq}_{b,H^+}; hence, Eq. 20 simplifies to:

$$D^{eff,CO_2}_{H^+} \frac{d^2 c_{H^+}}{dx^2} + k_{b,CO_2}\, c^{eq}_{b,H_2CO_3} \left(1 - \frac{c_{H^+}}{c^{eq}_{b,H^+}} \right) = 0 \quad [22]$$

Using the equilibrium Eq. 19, we can show that Eq. 22 can be also written as:

$$D^{eff,CO_2}_{H^+} \frac{d^2 c_{H^+}}{dx^2} + k_{f,CO_2}\, c^{eq}_{b,CO_2} \left(1 - \frac{c_{H^+}}{c^{eq}_{b,H^+}} \right) = 0 \quad [23]$$

The final simplification can be done by defining a concept called the *chemical reaction boundary layer*:

$$\frac{d^2}{dx^2} \left(\frac{c_{H^+}}{c^{eq}_{b,H^+}} \right) = \frac{1}{(\delta^{CO_2}_{r,H^+})^2} \left(\frac{c_{H^+}}{c^{eq}_{b,H^+}} - 1 \right) \quad [24]$$

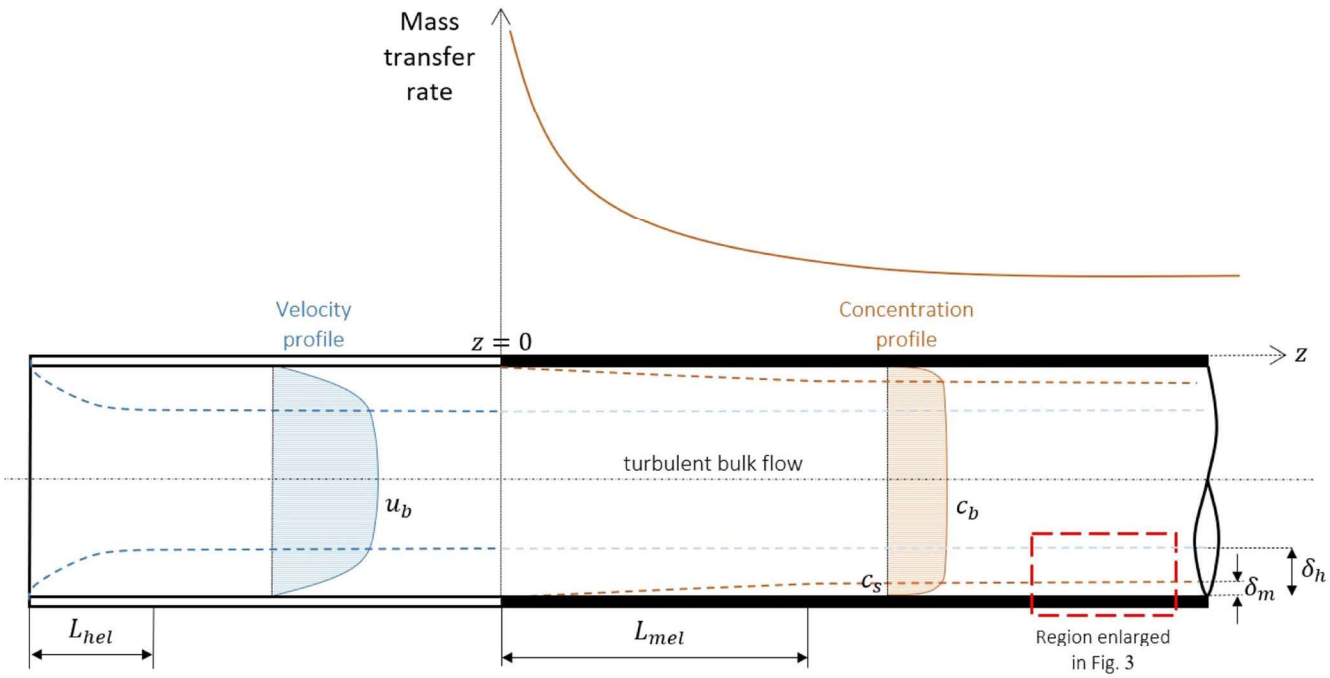

Figure 2. An illustration of velocity (u) and concentration (c) profiles in turbulent pipe flow (not drawn to scale), and the corresponding evolution of the hydrodynamic boundary layer (steady state thicknesses δ_h) and the mass transfer boundary layer (steady state thicknesses δ_m). The hydrodynamic boundary layer starts developing at the pipe inlet and is fully developed at the distance L_{hel} called the hydrodynamic entry length. Mass transfer starts evolving at $z = 0$ and is fully developed at the distance L_{mel} called the mass transfer entry length. The graph above shows the change of the mass transfer rate along the pipe, starting from the inlet. The region near the pipe surface for fully developed hydrodynamic and mass transfer conditions is indicated by a red box on the right and enlarged in Fig. 3.

where $\delta_{r,\mathrm{H^+}}^{\mathrm{CO_2}}$ has the dimension of length and is the thickness of the chemical reaction boundary layer for H^+ ions in aqueous CO_2-saturated solutions:

$$\delta_{r,\mathrm{H^+}}^{\mathrm{CO_2}} \equiv \sqrt{\frac{D_{\mathrm{H^+}}^{eff,\mathrm{CO_2}}\, c_{b,\mathrm{H^+}}^{eq}}{k_{f,\mathrm{CO_2}}\, c_{b,\mathrm{CO_2}}^{eq}}} \qquad [25]$$

The introduction of the *chemical reaction boundary layer* justifies a brief explanation. One of the first times this concept was introduced in the electrochemical literature was in the classical text by Vetter.[3,18,19] By definition, a *boundary layer* is a very thin region close to the metal surface where a given parameter (velocity, temperature, species concentration, *etc.*) changes from a value at the surface to that found in the bulk (see illustration in Fig. 2).[a] Beyond the edge of the boundary layer, *i.e.*, in the bulk, the parameter's value is considered to be constant. When that parameter is velocity, the boundary layer is called the *hydrodynamic boundary layer*; when the parameter is concentration, it is called the *mass transfer boundary layer* or interchangeably the *diffusion boundary layer*. For turbulent flow of aqueous species, the mass transfer boundary layer is much thinner and is deeply imbedded in the hydrodynamic boundary layer, as seen in Fig. 3 and Fig. 4. The difference in concentrations across the mass transfer boundary layer is usually caused by a relatively slow rate of mass transfer by molecular diffusion, between the *surface*—where the species is rapidly produced or consumed (in our case the H^+ ion) by a heterogeneous electrochemical reaction and the *bulk*—where convective mixing dominates, and the concentration profile is flat. When in addition to slow diffusion, there is a homogenous chemical reaction occurring throughout the solution, which effectively replenishes the reacting species (in our case H^+ ion), thereby maintaining equilibrium, the flat concentration profile extends much closer to the metal surface, as illustrated in Fig. 4. In this case, the changes in species concentration are limited to an even thinner region in the very proximity of the surface, where the consumption rate by the heterogeneous electrochemical reaction exceeds the production rate by the homogenous chemical reaction. This thin layer of the solution is called the *chemical reaction boundary layer*. For example, a typical thickness of a diffusion boundary layer in turbulent pipe flow of an aqueous solution is of the order of microns; the chemical reaction boundary layer in aqueous CO_2 solutions is usually an order of magnitude smaller.[16,17]

We can always think of the mass transfer boundary layer thickness $\delta_{m,\mathrm{H^+}}$ as one that would exist if there were no significant chemical reactions affecting the species concentration in the vicinity of the metal surface. Likewise, we can imagine that the thickness of the chemical reaction boundary layer $\delta_{r,\mathrm{H^+}}^{\mathrm{CO_2}}$ would be the one obtained in the absence of any convective mixing affecting the species concentrations. In reality, the actual thickness of the mass transfer boundary layer δ is a single and unique measure of the distance from the metal surface, over which there is a significant change in species concentration, and we cannot have two different measures of this distance, i.e., $\delta_{m,\mathrm{H^+}}$ and $\delta_{r,\mathrm{H^+}}^{\mathrm{CO_2}}$ to be true at the same time; the actual thickness of the mass transfer boundary layer δ is always equal to the smaller of the two:

$$\delta = \min\left(\delta_{m,\mathrm{H^+}},\, \delta_{r,\mathrm{H^+}}^{\mathrm{CO_2}}\right) \qquad [26]$$

Now, we can solve Eq. 24 by introducing a non-dimensional concentration ratio u:

$$u = \frac{c_{\mathrm{H^+}}}{c_{b,\mathrm{H^+}}^{eq}} \qquad [27]$$

Thus, Eq. 24 can be expressed as:

$$\frac{d^2u}{dx^2} = \frac{(u-1)}{(\delta_{r,\mathrm{H^+}}^{\mathrm{CO_2}})^2} \qquad [28]$$

This a second order linear heterogeneous differential equation, which can be solved analytically given the appropriate boundary conditions:

At the metal surface we can set:

$$\text{for } x = 0 \Rightarrow c_{\mathrm{H^+}} = c_{s,\mathrm{H^+}} \Rightarrow u = u_s \qquad [29]$$

where $u_s = c_{s,\mathrm{H^+}}/c_{b,\mathrm{H^+}}^{eq}$ is the non-dimensional surface concentration of H^+ ions.

At the edge of the diffusion boundary layer, it is assumed that the solution is thoroughly mixed, with the concentrations being the same as that in the bulk; hence we can write:

$$\text{for } x = \delta_{m,\mathrm{H^+}} \Rightarrow c_{\mathrm{H^+}} = c_{b,\mathrm{H^+}}^{eq} \Rightarrow u = 1 \qquad [30]$$

Solving the differential Eq. 28 with boundary conditions (29) and (30), will result in a solution of the form:

$$u(x) = (1-u_s)\left[\frac{\exp\left(\frac{x}{\delta_{r,\mathrm{H^+}}^{\mathrm{CO_2}}}\right)}{\exp\left(\frac{2\delta_{m,\mathrm{H^+}}}{\delta_{r,\mathrm{H^+}}^{\mathrm{CO_2}}}\right)-1} + \frac{\exp\left(-\frac{x}{\delta_{r,\mathrm{H^+}}^{\mathrm{CO_2}}}\right)}{\exp\left(-\frac{2\delta_{m,\mathrm{H^+}}}{\delta_{r,\mathrm{H^+}}^{\mathrm{CO_2}}}\right)-1}\right] + 1 \qquad [31]$$

The flux of H^+ ions at the metal surface in aqueous CO_2-saturated solutions can be expressed as:

$$N\big|_{x=0} \equiv -D_{\mathrm{H^+}}^{eff,\mathrm{CO_2}} \frac{dc_{\mathrm{H^+}}}{dx}\bigg|_{x=0} = -D_{H^+}^{eff,\mathrm{CO_2}}\, c_{b,\mathrm{H^+}}^{eq} \frac{du(x)}{dx}\bigg|_{x=0} \qquad [32]$$

So, by using Eq. 31, the flux will be equal to:

$$N\big|_{x=0} = -\frac{(1-u_s)\, D_{\mathrm{H^+}}^{eff,\mathrm{CO_2}}\; c_{b,H^+}^{eq}}{\delta_{r,\mathrm{H^+}}^{\mathrm{CO_2}}} \frac{\exp\left(\frac{2\delta_{m,\mathrm{H^+}}}{\delta_{r,\mathrm{H^+}}^{\mathrm{CO_2}}}\right)+1}{\exp\left(\frac{2\delta_{m,\mathrm{H^+}}}{\delta_{r,\mathrm{H^+}}^{\mathrm{CO_2}}}\right)-1} \qquad [33]$$

or in terms of $c_{\mathrm{H^+}}$ concentration:

$$N\big|_{x=0} = -\frac{(c_{b,\mathrm{H^+}}^{eq} - c_{s,\mathrm{H^+}}) D_{\mathrm{H^+}}^{eff,\mathrm{CO_2}}}{\delta_{r,\mathrm{H^+}}^{\mathrm{CO_2}}} \frac{\exp\left(\frac{2\delta_{m,\mathrm{H^+}}}{\delta_{r,\mathrm{H^+}}^{\mathrm{CO_2}}}\right)+1}{\exp\left(\frac{2\delta_{m,\mathrm{H^+}}}{\delta_{r,\mathrm{H^+}}^{\mathrm{CO_2}}}\right)-1}$$
$$= -\frac{(c_{b,\mathrm{H^+}}^{eq} - c_{s,\mathrm{H^+}}) D_{\mathrm{H^+}}^{eff,\mathrm{CO_2}}}{\delta_{r,\mathrm{H^+}}^{\mathrm{CO_2}}} coth\left(\frac{\delta_{m,\mathrm{H^+}}}{\delta_{r,\mathrm{H^+}}^{\mathrm{CO_2}}}\right) \qquad [34]$$

In a limiting current density scenario, when the rate of the overall electrochemical Reaction 5 is governed by the *rds* Reaction 1, all the H^+ ions that arrive at the metal surface by diffusion, Reaction 3, as well as those that are locally produced by the dissociation Reaction 2, are consumed almost instantaneously by the fast charge transfer Reaction 4; hence, the concentration of H^+ ions at the metal surface

[a]The edge of the boundary layer is defined as a location where the value of the hydrodynamic parameter reaches 90%, 95% or 99% of the bulk value (different values used in different texts[31–33]).

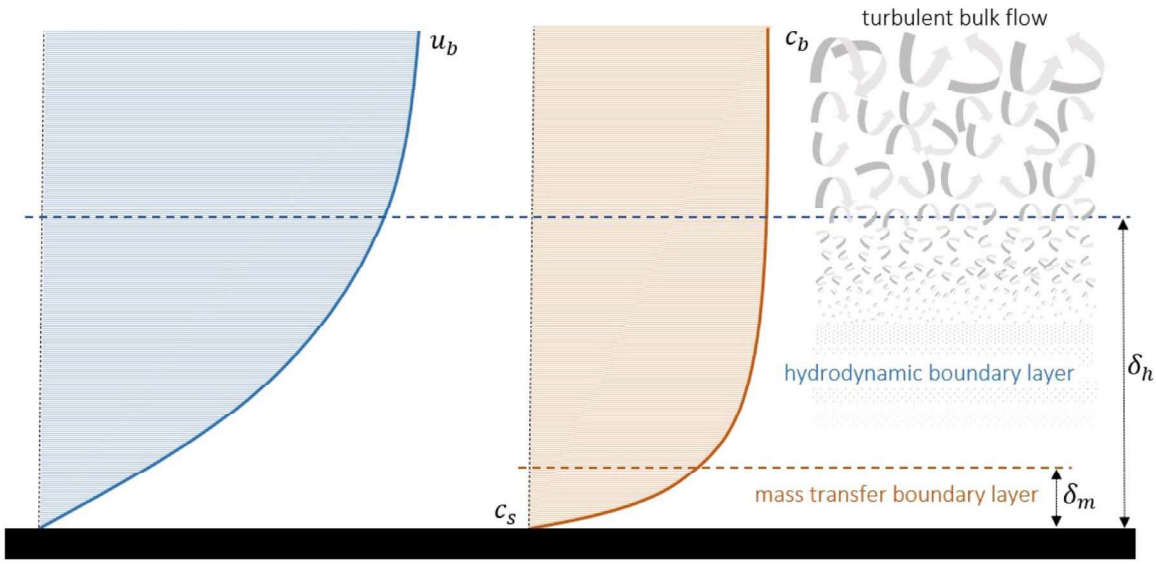

Figure 3. An enlargement of the region near a solid surface in fully developed turbulent flow (not drawn to scale) showing the decay of turbulent mixing as the surface is approached and the resulting velocity (u) and species concentration (c) profiles in relation to the hydrodynamic boundary layer thickness δ_h and the mass transfer boundary layer thickness δ_m.

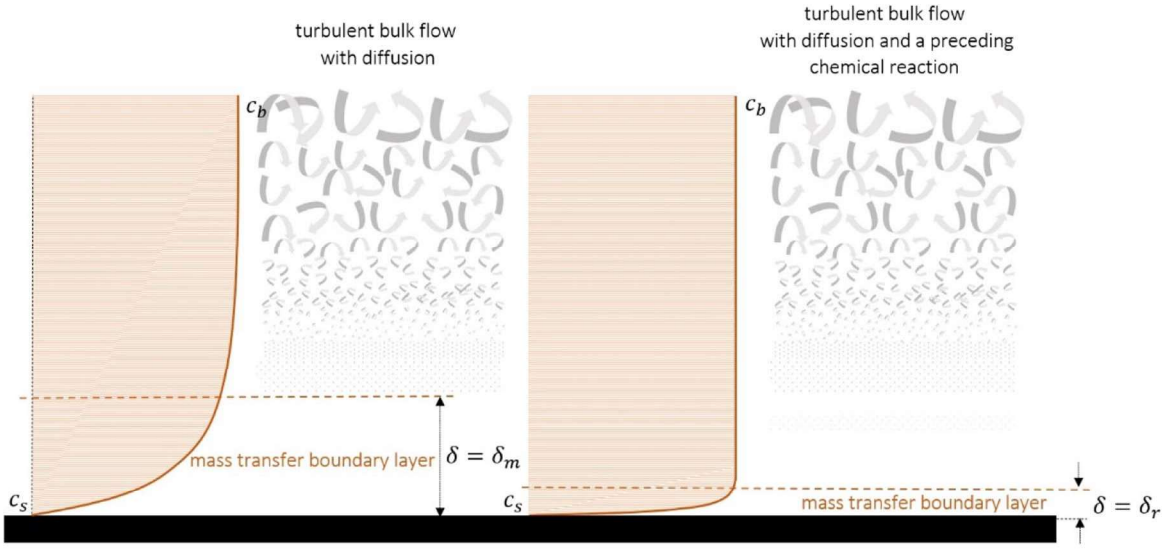

Figure 4. An illustration of species concentration profile in fully developed turbulent flow in relation to the mass transfer boundary layer thickness δ_m and chemical reaction boundary layer thickness δ_r. The actual thickness of the mass transfer boundary layer is δ (see Eq. 26).

approaches zero: $c_{H^+} \approx 0$. Then, we can set $c_{s,H^+} = 0$ in Eq. 34 and multiply the resulting flux by the Faraday constant F, in order to obtain the limiting current density[8] for the diffusion of H^+ ions with buffering due the presence of CO_2:

$$i_{lim,H^+}^{buff,CO_2} = \frac{F\, D_{H^+}^{eff,CO_2} c_{b,H^+}^{eq}}{\delta_{r,H^+}^{CO_2}} coth\left(\frac{\delta_{m,H^+}}{\delta_{r,H^+}^{CO_2}}\right) \quad [35]$$

By returning $\delta_{r,\,H^+}^{CO_2}$ from Eq. 25, we can derive an alternative expression for the limiting current density:

$$i_{lim,H^+}^{buff,CO_2} = F\sqrt{D_{H^+}^{eff,CO_2}\, k_{f,CO_2}\, c_{b,CO_2}^{eq}\, c_{b,H^+}^{eq}}\, coth\left(\frac{\delta_{m,\,H^+}}{\delta_{r,\,H^+}^{CO_2}}\right) \quad [36]$$

This is a general expression, which also holds at the limits. For example, when there is no CO_2 in the aqueous solution: $c_{b,CO_2}^{eq} = 0$ and therefore $c_{b,H_2CO_3}^{eq} = 0$, there is no buffering, and the resulting limiting current density should become equal to a pure diffusion limiting current density of H^+ ions. It can be easily shown that this is true, by taking a limit of Eq. 36 when $c_{b,CO_2}^{eq} \to 0$; this transforms Eq. 36 into Eq. 7 for pure mass transfer H^+ ion limiting current density.

Equation 36 is similar to Eq. 8, originally derived by Vetter's[3] with a modification for the flow effect introduced by Nesic et al.;[15] however, Eq. 36 is more general than expression (8), as it covers the effect of pH (via the c_{b,H^+}^{eq} term) in addition to the effect of CO_2 (via the c_{b,CO_2}^{eq} term).

In many cases, the term $coth(\delta_{m,H^+}/\delta_{r,H^+}^{CO_2})$, which accounts for the effect of flow, is close to 1; examples are stagnant solutions, low flow rates, and high temperatures; in these cases, Eq. 36 simplifies to:

$$i_{lim,\mathrm{H^+}}^{buff,\mathrm{CO_2}} = F\sqrt{D_{\mathrm{H^+}}^{eff,\mathrm{CO_2}}\, k_{f,\mathrm{CO_2}}\, c_{b,\mathrm{CO_2}}^{eq}\, c_{b,\mathrm{H^+}}^{eq}} \quad [37]$$

which reminds of the original Vetter's original equation[3] derived for stagnant solutions. This simpler version of the limiting current density equation covers a lot of practical scenarios; however, it is not sufficiently general and falters as the limits are approached. When there is no CO_2 in the aqueous solution, by setting $c_{b,\mathrm{CO_2}}^{eq} \to 0$ in Eq. 37, it gives $i_{lim,\mathrm{H^+}}^{buff,\mathrm{CO_2}} = 0$, what is obviously erroneous. Therefore, it is recommended to use the general expression given by Eq. 36, which now replaces the old and inadequate model represented by Eq. 9.

Implementation of the New Cathodic Limiting Current Density for Aqueous CO_2 Solutions

In calculation of the limiting current density via Eq. 36, a number of parameters need to be defined, such as: solution pH (*i.e.*, H^+ ion concentration), amount of dissolved CO_2 in solution, reaction rate constant for the CO_2 hydration reaction, flow geometry, and solution velocity, as well as key solution properties, such as: temperature, ionic strength, density, viscosity, and diffusivities of dissolved species. The implementation of the model presented here is focused on solutions that behave as ideal solutions or close to ideal solutions, up to approximately 3 wt.% salt. However, it has also been shown that the model predictions can be reasonably accurate in estimation of the limiting current density for concentrated brines up to 20 wt.% salt, when the effect of non-ideality is accounted for by using activity coefficients and the corrections for physical properties of the solution, which is a subject of a separate publication.[8]

There are many models for the calculation of solubility and speciation in aqueous CO_2 solutions. Some of them are relatively simple, while others are complex, particularly when it comes to non-ideal solutions.[8,34–40] The model presented below belongs to the first category.

For a solution with known pH, H^+ ion concentration can be simply calculated by using:

$$m_{b,\mathrm{H^+}}^{eq} = 10^{-pH} \quad [38]$$

where, m_{b,H^+}^{eq} is concentration of H^+ ion in the bulk solution in molality. In order to convert molality to molarity,[8] the solution density is required, which is given for aqueous NaCl solutions in the following text. For a solution with unknown pH, speciation calculations are required, which are described in detail for aqueous CO_2-saturated NaCl solutions elsewhere.[8,34,36,41]

The amount of dissolved CO_2 in an aqueous solution is usually obtained from a known CO_2 partial pressure in the gas phase, $p_{\mathrm{CO_2}}$. For an open system, such as a wet gas pipeline or a laboratory glass cell purged with CO_2 gas, in which $p_{\mathrm{CO_2}}$ can be assumed to be constant and explicitly known, one can simply use an equilibrium equation proposed by Oddo and Tomson.[34]

$$H_{CO_2} = \frac{c_{\mathrm{CO_{2(aq)}}}}{p_{\mathrm{CO_{2(g)}}}} \quad [39]$$

for the gas-liquid solubility reaction:

$$\mathrm{CO_{2(g)}} \overset{\mathrm{H_{CO_2}}}{\rightleftarrows} \mathrm{CO_{2(aq)}} \quad [40]$$

where, $c_{\mathrm{CO_2}}$ is the concentration of dissolved CO_2 in M. When $p_{\mathrm{CO_2}}$ is expressed in bar, then the Henry's constant in M/bar can be calculated from:

$$H_{\mathrm{CO_2}} = \frac{14.5}{1 + K_{hyd,\mathrm{CO_2}}} \times 10^{-(2.27+5.65\times10^{-3}\, T_f - 8.06\times10^{-6}\, T_f^2 + 0.075\, I)} \quad [41]$$

Here, T_f is the temperature in Fahrenheit, I is the solution ionic strength in molarity, and $K_{hyd,\,\mathrm{CO_2}}$ is the equilibrium constant fort the hydration Reaction 1. It should be noted that in the original publication of Oddo and Tomson,[34] the concentrations of $CO_{2(aq)}$ and H_2CO_3 are lumped together and therefore their Henry's constant is related to this lumped CO_2 concentration. The ratio $(1 + K_{hyd,\mathrm{CO_2}})$ is added to the original Oddo and Tomson[34] equation in order to calculate only the $CO_{2(aq)}$ concentration. Given that only 1 out of 500 dissolved CO_2 molecules is hydrated to give $H_2CO_{3(aq)}$ ($K_{hyd,\mathrm{CO_2}} \cong 0.002$ at 25 °C),[8,42] the impact of this correction will be very small on $CO_{2(aq)}$ concentration.

For closed systems, such as: oil pipelines, pressurized tanks, and laboratory autoclaves, the CO_2 solubility calculation is more complicated, as $p_{\mathrm{CO_2}}$ is not explicitly known and involves solving the gas-liquid equilibrium equation simultaneously with the aqueous equilibria equations and a mass balance equation for carbonic species.[8]

In order to calculate the effective diffusivity $D_{\mathrm{H^+}}^{eff,\mathrm{CO_2}}$, the diffusivities $D_{\mathrm{H^+}}$ and $D_{\mathrm{H_2CO_3}}$ in aqueous solutions are required. At 298.15 K and infinite dilution in water the values of $D_{\mathrm{H^+}}$ and $D_{\mathrm{H_2CO_3}}$ can be found in the open literature.[8,43] To correct the diffusion coefficients for temperature and NaCl concentration of interest the following equations can be used:[44,45]

$$\frac{D_{T,i}^{o}}{D_{298.15,i}^{o}} = \frac{T}{298.15} \times \frac{\mu_{298.15,\mathrm{H_2O}}}{\mu_{T,H_2O}} \exp\left(\frac{B_i}{T} - \frac{B_i}{298.15}\right) \quad [42]$$

$$\frac{D_i}{D_{T,i}^{o}} = 1 - K_i\sqrt{c_{\mathrm{NaCl}}} \quad [43]$$

where T is solution temperature in K, $\mu_{298.15,\mathrm{H_2O}}$ is dynamic viscosity of water at 298.15 K in Pa·s, $\mu_{T,\mathrm{H_2O}}$ is dynamic viscosity of water at temperature T in Pa·s, $D_{298.15,\,i}^{o}$ is diffusion coefficient of species i at 298.15 K and infinite dilution in water in $m^2\ s^{-1}$, $D_{T,i}^{o}$ is diffusion coefficient of species i at temperature T and infinite dilution in water in $m^2\ s^{-1}$, B_i is an adjustable constant for species i in K, c is concentration of NaCl aqueous solution in M, D_i is diffusion coefficient of species i at temperature T and supporting electrolyte concentration of c in $m^2\ s^{-1}$, and K_i is an adjustable coefficient for species i in NaCl aqueous solutions in $M^{-0.5}$. The values for H^+ ion and H_2CO_3 diffusivities at 298.15 K and infinite dilution in water as well as B_i and K_i for these species are given in Table I.

The forward and backward reaction rate constants for the hydration of dissolved CO_2, Reaction 1, in 1/s are taken from,[46] with minor corrections:

$$k_{f,\mathrm{CO_2}} = 3.22 \times 10^{11} \exp\left(-\frac{74011}{RT}\right) \quad [44]$$

$$k_{b,\mathrm{CO_2}} = 4.86 \times 10^{12} \exp\left(-\frac{64458}{RT}\right) \quad [45]$$

The equilibrium constant for the hydration of dissolved CO_2, Reaction 1 is then:

$$K_{hyd,CO_2} = \frac{k_{f,\mathrm{CO_2}}}{k_{b,\mathrm{CO_2}}} = 6.62 \times 10^{-2} \exp\left(-\frac{9553}{RT}\right) \quad [46]$$

where R= 8.3145 J mol^{-1} K^{-1} is the gas constant and T is the solution temperature in K.

Once these values are known, $\delta_{r,\,\mathrm{H^+}}^{\mathrm{CO_2}}$ in m can be calculated from Eq. 25. The thickness of the mass transfer boundary layer for H^+ ions can be found from:

Table I. Diffusion coefficient at 298.15 K and infinite dilution in water and constants used in Eqs. 42 and 43 for H^+ ion and H_2CO_3.

Species i	H^+	H_2CO_3	References
$D^o_{298.15,i}$ ($m^2\ s^{-1}$)	9.312×10^{-9}	1.465×10^{-9}	8,43
B_i	837.79	0	8,44
K_i ($M^{-0.5}$)	0.271	0.151	8

$$\delta_{m,H^+} = \frac{D_{H^+}}{k_{m,H^+}} \quad [47]$$

where k_{m,H^+} is the mass transfer coefficient for H^+ ions in an aqueous solution in m s^{-1} and depends on the flow geometry as well as the flow velocity. Typically, for a given flow geometry, one can find k_{m,H^+} from an empirical mass transfer correlation, defined for that geometry, in terms of a nondimensional Sherwood number:

$$Sh_{H^+} = \frac{k_{m,H^+}L}{D_{H^+}} = a\, Re^x Sc^y \quad [48]$$

where L is the characteristic dimension for the flow geometry of interest (e.g., pipe diameter, or cylinder diameter, etc.) in m, while a, x, and y are empirical constants determined for that flow geometry.[31,47–49] For example, for a pipe geometry, $a = 0.0165$, $x = 0.86$, and $y = 0.33$[48] or for a rotating cylinder, $a = 0.0791$, $x = 0.7$, and $y = 0.356$.[47] The nondimensional Reynolds number is defined as:

$$Re = \frac{\rho_{sol} V L}{\mu_{sol}} = \frac{VL}{\nu_{sol}} \quad [49]$$

where, V is the bulk velocity in m s^{-1}, ρ_{sol} is the aqueous solution density in kg m^{-3}, μ_{sol} is the solution dynamic viscosity in Pa·s and $\nu_{sol} = \mu_{sol}/\rho_{sol}$ is the solution kinematic viscosity in $m^2\ s^{-1}$.

The nondimensional Schmidt number is defined as:

$$Sc_{H^+} = \frac{D_{H^+}}{\nu_{sol}} \quad [50]$$

The density and viscosity of an aqueous solution depend primarily on temperature and dissolved salt concentration. The density and viscosity of aqueous NaCl solutions can be calculated by using the Batzle and Wang model:[50]

$$\rho_{H_2O} = 1 + 1 \times 10^{-6}(-80T_c - 3.3T_c^2 + 0.00175T_c^3 + 489P - 2T_cP + 0.016T_c^2P - 1.3 \times 10^{-5}T_c^3P - 0.333P^2 - 0.002\,T_cP^2) \quad [51]$$

$$\rho_{sol} = \rho_{H_2O} + S[0.668 + 0.44S + 10^{-6} \times (300P - 2400PS + T_c(80 + 3T_c - 3300S - 13P + 47PS))] \quad [52]$$

$$\mu_{sol} = 10^{-4} + 3.33 \times 10^{-4}S + 10^{-3}(1.65 + 91.9S^3) \times \exp\left(-(0.42(S^{0.8} - 0.17)^2 + 0.045)T_c^{0.8}\right) \quad [53]$$

where ρ_{H_2O} and ρ_{sol} are the pure water and the aqueous NaCl solution density in g cm^{-3}, respectively, T_c is the solution temperature in °C, P is the total pressure in MPa, μ_{sol} is the dynamic viscosity of the aqueous NaCl solution in Pa·s, and S is the salt weight (mass) fraction calculated as:

$$S = \frac{m_{salt}}{m_{water} + m_{salt}} \quad [54]$$

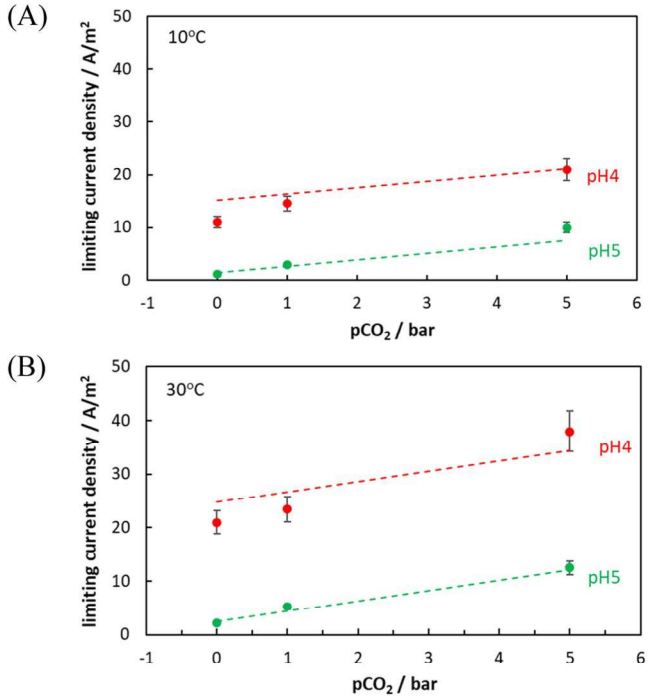

Figure 5. The limiting current density for H^+ ion reduction in CO_2-saturated aqueous solutions as a function of CO_2 partial pressure, for pH4 and pH5, at 10 °C (A) and 30 °C (B). Dashed lines are obtained using the new model. Points are experimental values obtained by Kahyarian et al.[7] in turbulent flow through a thin channel with a thickness of 3.57 mm and a flow velocity of 12.9 m s^{-1}, using 0.1 M NaCl aqueous CO_2-saturated solution. Error bars are obtained by accounting for the data scatter in the original measurements.

where, m_{salt} is the mass of salt and m_{water} is the mass of water in the solution.

Verification of the New Cathodic Limiting Current Density for Aqueous CO_2 Solutions

In order to check the performance of the proposed model for calculating the limiting current density in aqueous CO_2-saturated solutions, the most accurate experimental data were sought.[7,8,46,51,52] The selected data were demonstrably reproducible, had a low margin of experimental error and have covered a broad range of conditions: $p_{CO_2} = 0 - 15$ bar, pH3—pH6, T = 10–80 °C, and NaCl concentrations 0–1 wt.%. They came from four different flow setups: rotating disk flow, rotating cylinder flow, pipe flow, and flow between parallel plates (total of 32 experiments) and involved DC potentiodynamic polarization measurements. To the best of our knowledge, there are no similar studies that were done using transient techniques such as EIS or EHD that would provide additional experimental data useful in this verification. The existing studies using EIS and EHD are either pure theoretical models of the CE mechanism,[22] or they are limited to determining transport properties of electrolytes in pure mass transfer controlled systems, such as diffusion coefficient or Schmidt number.[53,54]

The few graphs presented below indicate the performance of the model. A sample comparison presented in Fig. 5 shows that the model captures the increasing trend in the limiting current density with p_{CO_2}. The calculated values are close to the measured ones, in many cases passing within the error bars, which represent the scatter in the measurements. Similar increasing trends were obtained with temperature and velocity and a decreasing trend was seen with pH, as would be expected.

A more comprehensive comparison can be seen in the parity plot shown in Fig. 6, which shows all the experimental data points used. The calculations were done by using both the old model, where the limiting current density was obtained with Eq. 9, and the new model

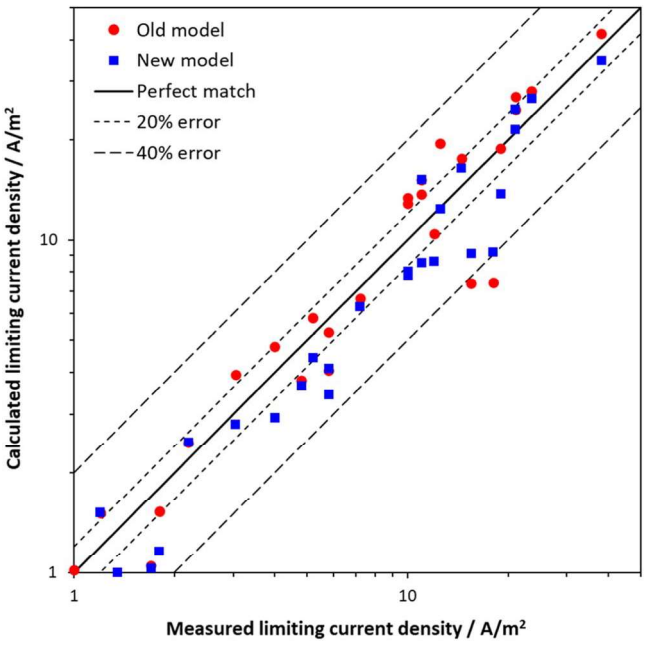

Figure 6. A parity plot showing the comparison between the measured limiting current densities and the calculated ones, for a variety of conditions covering a broad range of conditions: p_{CO_2} = 0–15 bar, pH3—pH6, T = 10 °C–80 °C, and coming from four different flow setups: rotating disk flow, rotating cylinder flow, pipe flow, and flow between parallel plates.[7,8,46,51,52] The red circles represent the old model where the calculations were done using Eq. 9 and the blue squares represent the new model using Eq. 36.

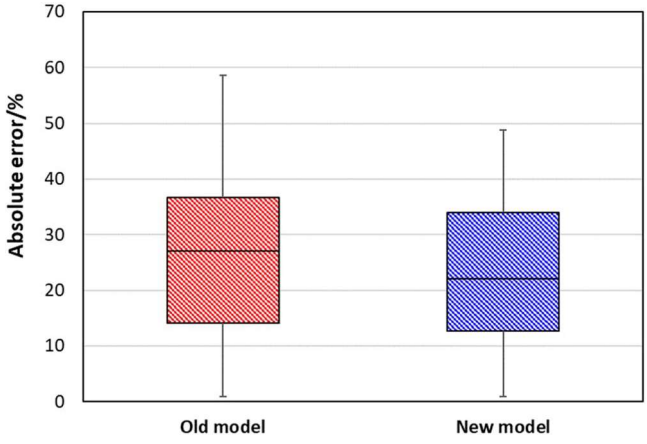

Figure 7. Comparison between the old and the new equations for calculating the limiting current density in aqueous CO_2-saturated solution shown by a box-and-whisker plot (min, quartile 1, median, quartile 3, and max).

which is based on Eq. 36. It can be argued that both models performed quite well overall and that, from this graph, it is difficult to state that one is more accurate than the other. This can be better seen in Fig. 7, where the error metrics for the two models are shown in the form of a "box and whiskers" plot. When compared to the measured values it appears that the new model has slightly better accuracy as it has a slightly lower mean error and an overall smaller spread. However, the key point is that the new model is based on the corrected cathodic reaction mechanism, while the old model is not. There is a good reason why the old model gives reasonable predictions: it also includes co-diffusion of H^+ and H_2CO_3, just like the new model does; however, in the old model this co-diffusion happens without any chemical reactions between them, i.e., each species diffuses independently from the other, what is not physically correct. This was corrected in the new model.

Conclusions

The following are the major conclusions reached in this study:

- A new approach for calculating the limiting current density for the H^+ reduction reaction in aqueous CO_2 solutions is proposed.
- The new model is based on the recently corrected mechanism for the cathodic reactions in aqueous CO_2 solutions.
- The new model relies on solving the co-diffusion of H^+ and H_2CO_3 in the mass transfer boundary layer, with a simultaneous homogeneous chemical reaction.
- The performance of the new model is successfully validated by comparing it with experimental data which were demonstrably reproducible, had a low margin of experimental error and covered a broad range of conditions.

ORCID

Fazlollah Madani Sani https://orcid.org/0000-0002-9689-8868

References

1. J. O. Bockris and A. K. N. Reddy, *Modern Electrochemistry: An Introduction to an Interdisciplinary area, a Plenum/Rosetta* (New York, NY)(Plenum Publishing Corporation) 2 (1973).
2. E. Brunner, "Reaktionsgeschwindigkeit in heterogenen systemen." *Z. Für Phys. Chem.*, **47U**, 56 (1904).
3. K. J. Vetter, *Electrochemical Kinetics: Theoretical and Experimental Aspects* (New York)(Academic) (1967).
4. C. de Waard and D. E. Milliams, "Carbonic acid corrosion of steel." *Corrosion*, **31**, 177 (1975).
5. G. Schmitt and B. Rothmann, "Untersuchungen zum korrosionsmechanismus von unlegiertem stahl in sauerstofffreien kohlensäurelösungen. teil i. kinetik der Wasserstoffabscheidung." *Mater. Corros.*, **28**, 816 (1977).
6. L. G. S. Gray, B. G. Anderson, M. J. Danysh, and P. R. Tremaine, "Mechanisms of carbon steel corrosion in brines containing dissolved carbon dioxide at pH 4." *CORROSION*(New Orleans, LA)(NACE International) p. 464 (1989).
7. A. Kahyarian and S. Nesic, "A new narrative for CO_2 corrosion of mild steel." *J. Electrochem. Soc.*, **166**, C3048 (2019).
8. F. Madani Sani, "The effect of salt concentration on aqueous strong acid, carbon dioxide, and hydrogen sulfide corrosion of carbon steel." *PhD Dissertation*, Ohio University (2021).
9. B. E. Conway and B. V. Tilak, "Interfacial processes involving electrocatalytic evolution and oxidation of H_2, and the role of chemisorbed H." *Electrochim. Acta*, **47**, 3571 (2002).
10. L. J. Vracar and D. M. Drazic, "Influence of chloride ion adsorption on hydrogen evolution reaction on iron." *J. Electroanal. Chem.*, **339**, 269 (1992).
11. C. de Waard and D. E. Milliams, "Prediction of carbonic acid corrosion in natural gas pipelines." *Int Conf Intern Extern. Prot Pipes.*, **1**, F1-1 (1975).
12. E. Remita, B. Tribollet, E. Sutter, V. Vivier, F. Ropital, and J. Kittel, "Hydrogen evolution in aqueous solutions containing dissolved CO_2: Quantitative contribution of the buffering effect." *Corros. Sci.*, **50**, 1433 (2008).
13. T. Tran, B. Brown, and S. Nesic, "Corrosion of mild steel in an aqueous CO_2 environment—basic electrochemical mechanisms revisited." *CORROSION*(Dallas, TX)(NACE International) p. 5671 (2015).
14. L. G. S. Gray, B. G. Anderson, M. J. Danysh, and P. R. Tremaine, "Effect of pH and temperature on the mechanism of carbon steel corrosion by aqueous carbon dioxide." *CORROSION*(Las Vegas, NV)(NACE International) p. 40 (1990).
15. S. Nesic, B. F. M. Pots, J. Postlethwaite, and N. Thevenot, "Superposition of diffusion and chemical reaction controlled limiting currents- application to CO_2 corrosion." *J. Corros. Sci. Eng.*, **1**, 3 (1995).
16. S. Nesic, "Carbon dioxide corrosion of mild steel." *Uhligs Corrosion Handbook*, ed. R. W. Revie (New York, NY)(Wiley) 3rd ed. p. 229 (2011).
17. S. Nesic and W. Sun, "2.25 - Corrosion in Acid Gas Solutions." *Shreir's Corrosion*, ed. B. Cottis, M. Graham, R. Lindsay, S. Lyon, T. Richardson, D. Scantlebury, and H. Stott (Oxford)(Elsevier) 2, 1270 (2010).
18. J. Koutecky and V. G. Levich, "The application of the rotating disk electrode to studies of kinetic and catalytic processes." *Zhurnal Fiz. Khimii.*, **32**, 1565 (1958).
19. R. R. Dogonadze, "The application of the rotating disk electrode to studies of kinetic and catalytic processes in electrochemistry- The case of different diffusion coefficients." *Zhurnal Fiz. Khimii.*, **32**, 2437 (1958).
20. P. H. Rieger, *Electrochemistry* (New York, NY)(Chapman and Hall) 2nd ed. (1994).
21. P. H. M. Leal, N. A. Leite, P. R. P. Viana, F. V. V. de Sousa, O. E. Barcia, and O. R. Mattos, "Numerical analysis of the steady-state behavior of CE processes in rotating disk electrode systems." *J. Electrochem. Soc.*, **165**, H466 (2018).

22. P. H. M. Leal, O. E. Barcia, and O. R. Mattos, "Numerical analysis of CE processes in RDE systems: diffusion and electro-hydrodynamic impedances." *J. Electrochem. Soc.*, **167**, 026502 (2020).
23. M. S. Harding, B. Tribollet, V. Vivier, and M. E. Orazem, "The influence of homogeneous reactions on the impedance response of a rotating disk electrode." *J. Electrochem. Soc.*, **164**, E3418 (2017).
24. J. M. Hale, "Transients in convective systems: I. Theory of galvanostatic, and galvanostatic with current reversal transients, at a rotating disc electrode." *J. Electroanal. Chem.*, **6**, 187 (1963).
25. M. Nordsveen, S. Nesic, R. Nyborg, and A. Stangeland, "A mechanistic model for carbon dioxide corrosion of mild steel in the presence of protective iron carbonate films—Part 1: theory and verification." *Corrosion*, **59**, 443 (2003).
26. S. Nesic, M. Nordsveen, R. Nyborg, and A. Stangeland, "A mechanistic model for carbon dioxide corrosion of mild Steel in the presence of protective iron carbonate films Part—2: a numerical experiment." *Corrosion*, **59**, 489 (2003).
27. S. Nesic and K.-L. J. Lee, "A mechanistic model for carbon dioxide corrosion of mild steel in the presence of protective iron carbonate films—Part 3: film growth model." *Corrosion*, **59**, 616 (2003).
28. A. J. Bard and L. R. Faulkner, *Electrochemical Methods: Fundamentals and Applications* (New York, NY)(John Wiley & Sons) 2nd ed. (2000).
29. H. Matsuda, "Theory of stationary current-voltage curves of redox-electrode reactions in hydrodynamic voltammetry: VI. Ring electrodes." *J. Electroanal. Chem. Interfacial Electrochem.*, **35**, 77 (1972).
30. H. Matsuda, "Theory of stationary current-voltage curves of redox-electrode reactions in hydrodynamic voltammetry: VII. Stationary disk and ring electrodes in a uniformly rotating fluid." *J. Electroanal. Chem. Interfacial Electrochem.*, **38**, 159 (1972).
31. F. Opekar and P. Beran, "Rotating disk electrodes." *J. Electroanal. Chem. Interfacial Electrochem.*, **69**, 1 (1976).
32. D. P. Gregory and A. C. Riddiford, "Transport to the surface of a rotating disc." *J. Chem. Soc. Resumed.*, **731**, 3756 (1956).
33. H. Schlichting (Deceased) and K. Gersten, *Boundary-Layer Theory* (Berlin) (Springer) 9th ed. (2017).
34. J. E. Oddo and M. B. Tomson, "Simplified calculation of $CaCO_3$ saturation at high temperatures and pressures in brine solutions." *J. Pet. Technol.*, **34**, 1583 (1982).
35. F. J. Millero, "Thermodynamics of the carbon dioxide system in the oceans." *Geochim. Cosmochim. Acta*, **59**, 661 (1995).
36. X. Gao, F. Madani Sani, Z. Ma, B. Brown, M. Singer, and S. Nesic, "A quantitative study of $FeCO_3$ solubility in non-ideal solutions." *AMPP Conference & Expo* (Virtual) p. 16964 (2021).
37. N. Spycher, K. Pruess, and J. Ennis-King, "CO_2-H_2O mixtures in the geological sequestration of CO_2. i. assessment and calculation of mutual solubilities from 12 ° C to 100 °C and up to 600 bar." *Geochim. Cosmochim. Acta*, **67**, 3015 (2003).
38. Z. Duan and D. Li, "Coupled phase and aqueous species equilibrium of the H_2O–CO_2–NaCl–$CaCO_3$ system from 0 °C to 250 °C, 1 to 1000 bar with NaCl concentrations up to saturation of halite." *Geochim. Cosmochim. Acta*, **72**, 5128 (2008).
39. S. Mao, D. Zhang, Y. Li, and N. Liu, "An improved model for calculating CO_2 solubility in aqueous NaCl solutions and the application to CO_2–H_2O–NaCl fluid inclusions." *Chem. Geol.*, **347**, 43 (2013).
40. R. D. Springer, P. Wang, and A. Anderko, "Modeling the properties of H_2S/CO_2/salt/water systems in wide ranges of temperature and pressure." *SPE J.*, **20**, 1,120 (2015).
41. D. Li and Z. Duan, "The speciation equilibrium coupling with phase equilibrium in the H_2O–CO_2–NaCl system from 0 °C to 250 °C, from 0 to 1000 bar, and from 0 to 5 molality of NaCl." *Chem. Geol.*, **244**, 730 (2007).
42. D. A. Palmer and R. V. Eldik, "The chemistry of metal carbonato and carbon dioxide complexes." *Chem. Rev.*, **83**, 651 (1983).
43. J. Newman and K. E. Thomas-Alyea, *Electrochemical Systems* (New York)(Wiley-Interscience) 3rd ed. (2004).
44. A. Anderko and M. M. Lencka, "Computation of electrical conductivity of multicomponent aqueous systems in wide concentration and temperature ranges." *Ind. Eng. Chem. Res.*, **36**, 1932 (1997).
45. M. Ciszkowska, Z. Stojek, S. E. Morris, and J. G. Osteryoung, "Steady-state voltammetry of strong and weak acids with and without supporting electrolyte." *Anal. Chem.*, **64**, 2372 (1992).
46. A. Kahyarian and S. Nesic, "On the mechanism of carbon dioxide corrosion of mild steel: experimental investigation and mathematical modeling at elevated pressures and non-ideal solutions." *Corros. Sci.*, **173**, 108719 (2020).
47. M. Eisenberg, C. W. Tobias, and C. R. Wilke, "Ionic mass transfer and concentration polarization at rotating electrodes." *J. Electrochem. Soc.*, **101**, 306 (1954).
48. F. P. Berger and K. F. F. L. Hau, "Mass transfer in turbulent pipe flow measured by the electrochemical method." *Int. J. Heat Mass Transf.*, **20**, 1185 (1977).
49. C. A. Sleicher and M. W. Rouse, "A convenient correlation for heat transfer to constant and variable property fluids in turbulent pipe flow." *Int. J. Heat Mass Transf.*, **18**, 677 (1975).
50. M. Batzle and Z. Wang, "Seismic properties of pore fluids." *Geophysics*, **57**, 1396 (1992).
51. F. Madani Sani, B. Brown, and S. Nesic, "A mechanistic study on the effect of salt concentration on uniform corrosion rate of pipeline steel in acidic aqueous environments." *AMPP Conference & Expo* (Virtual) p. 16788 (2021).
52. S. Nesic, G. T. Solvi, and J. Enerhaug, "Comparison of the rotating cylinder and pipe flow tests for flow-sensitive carbon dioxide corrosion." *Corrosion*, **51**, 773 (1995).
53. B. Robertson, B. Tribollet, and C. Deslouis, "Measurement of diffusion coefficients by DC and EHD electrochemical methods." *J. Electrochem. Soc.*, **135**, 2279 (1988).
54. B. Tribollet, J. Newman, and W. H. Smyrl, "Determination of the diffusion coefficient from impedance data in the low frequency range." *J. Electrochem. Soc.*, **135**, 134 (1988).